Image to Volume Weighting Generalized ASSR for Arbitrary Pitch 3D and Phase–Correlated 4D Spiral Cone–Beam CT Reconstruction

Marc Kachelrieß*, Theo Fuchs, Robert Lapp, Dirk–Alexander Sennst, Stefan Schaller, Willi Kalender

Abstract— **The next generation of medical CT scanners will measure up to 16 slices or more simultaneously which will require dedicated cone–beam reconstruction algorithms. The basic requirements for medical CT are high image quality and fast reconstruction (reconstruction of a complete volume within a few minutes is desired). Due to the small cone–angle (typically a few degrees only) approximate cone–beam reconstruction will be the method of choice. A very promising candidate is the advanced single–slice rebinning (ASSR) which rebins the cone–beam data to parallel beam data on tilted reconstruction planes (R–planes) and utilizes 2D reconstruction algorithms to obtain tilted images [Med. Phys. 27(4), 754–772 (2000)].**

In its original form ASSR allows to reconstruct 3D data for a fixed pitch obtained with a non–tilted gantry. However, medical demands are manifold: the pitch must be freely selectable, gantry tilt scans are required and, last but not least, cardiac applications require phase–correlated 4D reconstructions. We have therefore generalized the ASSR algorithm by adding the following three attributes: a) the table increment per rotation is now correctly taken into account as the vector $\boldsymbol{d}$, b) the restriction on the optimality of the R–planes is loosened to allow for more than one R–plane per reconstruction position and c) the final volume is generated using adjustable weigths for the tilted images. These weights are used to balance between image quality and dose usage and to select a desired cardiac phase in the final volume. This (tilted) image to (cartesian) volume (I2V) weighting approach can be performed in real–time. To evaluate the new method we have simulated cone–beam rawdata of a thorax and a cardiac motion phantom.

The generalized ASSR approach in combination with I2V shows very good results even for low pitch ($p < 1.5$) scans. Since slightly more artifacts appear for the low pitch case with full dose usage (equal weights for all planes) it is necessary to provide real–time access to the weights. The cardiac reconstructions are of high image quality but slightly lower temporal resolution as compared to the gold standard 180°MCI.

Keywords— **Computed tomography (CT), Cone–beam Spiral CT (CBCT), 3D reconstruction, 4D reconstruction**

I. Introduction

FUTURE medical CT scanners will scan significantly more than four slices simultaneously. Major CT manufacturers have announced scanners of up to 16 slices for the end of 2001. Neglecting the cone–angle of the scanner as it is done in today's 4–slice reconstruction algorithms will then yield unacceptable image artifacts [1]. Therefore, there is a need for fast and efficient cone–beam reconstruction algorithms. Although a large number of more or less efficient algorithms have been developed in the last decade [2], none of them meets all requirements of medical CT: a) correct handling of the gantry tilt, b) arbitrary spiral pitch while using the full detector area and c) the ability of performing a 4D cardiac reconstruction. Whereas the gantry tilt problem can be solved in principle for all the existing algorithms by simply reformulating the coordinate transformations solving the other restrictions is not straightforward.

We therefore generalize the ASSR (advanced single–slice rebinning) algorithm [3] to fulfill these requirements. The ASSR algorithm, as an advancement of Noo's single–slice rebinning algorithm [4], fits tilted reconstruction planes to the spiral trajectory to perform a rebinning from the 3D cone–beam data to 2D parallel–beam data on these R–planes. The reconstruction then uses a standard 2D method (e.g. filtered backprojection) and the set of reconstructed tilted images is interpolated in the z–direction to obtain the final volume [3] (a similar method which has never been evaluated was proposed in [5]). Since ASSR has turned out to be very promising [6], [7] two generalizations thereof have been proposed: one for the case of arbitrary gantry tilt [8] and one to allow for arbitrary pitch [9]. The results are encouraging and led to the development of an even further generalization to combine these approaches. The new approach presented here uses the rebinning equations of reference [8] together with the idea to losen the restriction of the R–planes to allow for more than one R–plane per reconstruction position [9]. A novel idea of our approach is to weight each available image before it is interpolated into the final volume. The weights can be chosen to trade off between high image quality and high noise (i.e. assigning smaller weights to R–planes which are less optimal) or lower image quality and lower noise (i.e. assigning the same weight for each plane regardless of its optimality).

As a spin–off, the generalized ASSR combined with I2V allows to perform 4D reconstructions for low pitch scans with periodically moving objects. The weights of images corresponding to cardiac phases which should not appear in the volume are simply set to zero. Details of cardiac CT scanning and the restrictions on the maximum pitch as a function of the patient's heart rate can be found in references [10], [11], [12].

In this paper, we will outline the generalized ASSR algorithm and the weight selection and give some descriptive examples.

Institute of Medical Physics, University of Erlangen–Nürnberg, Krankenhausstr. 12, 91054 Erlangen. Corresponding author: Marc Kachelrieß, E–mail: marc.kachelriess@imp.uni–erlangen.de

II. Simulations

To evaluate our new approach we have simulated spiral cone–beam data corresponding to the in–plane geometry of a typical medical CT Scanner (1160 projections per rotation, 672 detector channels per detector row, and a fan angle $\Phi = 52°$) using a dedicated x–ray simulation tool (ImpactSim, VAMP GmbH, Möhrendorf, Germany). Two phantoms have been simulated: the thorax phantom described in the phantom data base http://www.imp.uni–erlangen.de/forbild and the cardiac motion phantom described in [11].

For the thorax scan in standard mode we have chosen a collimation of 16×1 mm and we have performed simulations for 4 mm, 8 mm, 16 mm and 24 mm table increment per rotation.

Since shorter rotation times and thinner slices are expected for the future we have simulated the cardiac motion phantom for a wide range of heart rates f_{H} with 0.375 s rotation time (160 rpm), 12×0.5 mm collimation and a table increment of $d = 2$ mm. This allows to cover the heart (typically 12 cm to 15 cm axial length) within less than 30 s (single breath–hold). Evaluating the thorax phantom in cardiac mode yields too huge data sets due to the highly overlapping and fine sampling in z. Thus we scaled the thorax scan by a factor of 2 in the z–direction, i.e. 12×1 mm and $d = 4$ mm (even so, the rawdata file size is 2.5 Gigs).

III. Reconstruction

The reconstructions shall be centered about the views $n\Delta\alpha_{\mathrm{R}}$ where $\Delta\alpha_{\mathrm{R}}$ is the so–called reconstruction increment and should be chosen small enough to ensure full detector usage and resolution [3]. The integer n counts the reconstruction positions. For each reconstruction position α_{R} an optimal R–plane which minimizes the mean square deviation Δ_{mean} of the plane to the spiral trajectory within the interval $\alpha_{\mathrm{R}} - \pi/2$ to $\alpha_{\mathrm{R}} + \pi/2$ can be computed [8]. Using these planes only, reconstruction for low pitch would be possible, but parts of the detector would remain unused and thus would have to be collimated out. Since we want to be able to use the full detector, our new approach allows to reconstruct more than one tilted image from a given reconstruction position. Assuming M images per reconstruction position the set of all R–planes is given (in normal representation) as

$$\mathrm{R}_{nm} : \boldsymbol{n}_{nm} \cdot \boldsymbol{r} - a_{nm} = 0$$

with $m = 1, \ldots, M$. The a_{nm} are chosen equidistant in m as $a_{nm} = a_n + m\Delta a_M$. The increments $\Delta\alpha_{\mathrm{R}}$ and Δa_M together with the value of M are chosen to ensure full detector usage. The normal vectors $\boldsymbol{n}_{nm}$ are chosen for a given a_{nm} to minimize the mean square deviation

$$\Delta^2_{nm} = \frac{1}{\pi} \int_{\alpha_{\mathrm{R}} - \frac{1}{2}\pi}^{\alpha_{\mathrm{R}} + \frac{1}{2}\pi} d\alpha \left(\boldsymbol{n}_{nm} \cdot \boldsymbol{s}(\alpha) - a_{nm}\right)^2$$

with $\boldsymbol{s}(\alpha)$ being the spiral source trajectory and $\alpha_{\mathrm{R}} = n\Delta\alpha_{\mathrm{R}}$. The minimization procedure is described in [8].

IV. Image Weights

We make use of two possibilities of weighting the individual images prior to volume interpolation. For a standard reconstruction, the image weights are chosen as

$$w_{nm} = \left(\frac{1}{\Delta_{nm}}\right)^q \quad \text{with} \quad q \geq 0\,.$$

The quality parameter q is used to balance between best dose usage ($q = 0$, making full use of non–optimal R–planes) and best image quality ($q = \infty$, only using the optimal R–planes and neglecting non–optimal ones).

For cardiac 4D reconstruction we additionally use the cardiac phase $c(\alpha) \in [0, 1)$, which is a function of the view angle α and describes the cardiac motion relative to R-R, to weight the images. The user desires to reconstruct the images at the reconstruction phase c_{R}. The mean square deviation of the cardiac phases contributing to reconstruction position $\alpha_{\mathrm{R}} = n\Delta\alpha_{\mathrm{R}}$ from the target phase c_{R} is defined as

$$\Delta^2_n = \frac{1}{\pi} \int_{\alpha_{\mathrm{R}} - \frac{1}{2}\pi}^{\alpha_{\mathrm{R}} + \frac{1}{2}\pi} d\alpha \left(c(\alpha) - c_{\mathrm{R}}\right)^2 .$$

Here, we implicitly assume a proper handling of the modulo property of the cardiac phase. We define the cardiac weight as

$$w_n = \left(\frac{1}{\Delta_n}\right)^{q'} \quad \text{with} \quad q' \geq 0$$

and again we have a quality parameter available to adjust the image quality.

V. Image to Volume Weighting

The final step is to perform an interpolation from a set $\{f_{nm}(x, y, z)\}$ of tilted images (each with weight w_{nm}) to a cartesian volume $f(x, y, z)$. In general, this can be achieved by convolving the reconstructed planes with a three dimensional interpolation kernel $k(x, y, z)$ followed by proper normalization:

$$f(x, y, z) = \frac{\sum_{nm} w_{nm} f_{nm}(x, y, z) * k(x, y, z)}{\sum_{nm} w_{nm} 1_{nm}(x, y, z) * k(x, y, z)}\,. \qquad (1)$$

The indicator function 1_{nm} is 1 if $(x, y, z) \in \mathrm{R}_{nm}$ and 0 elsewhere. Since ASSR does not require interpolations between image pixels in the x and y direction, the interpolation kernel reduces to a function of z only: $k(z)$. Its shape is currently chosen triangular and care is taken that the z–kernel is wide enough to avoid gaps in the final volume: the denominator of (1) must be positive $\forall\, x, y, z$. Using local kernels $k(x, y, z, x_0, y_0, z_0)$ and spatially varying weights $w_{nm}(x, y, z)$ may be of advantage but is not discussed here because this is beyond this short paper's scope. More sophisticated I2V methods such as modifying the kernel and the weights as a function of the cardiac information are under further investigation.

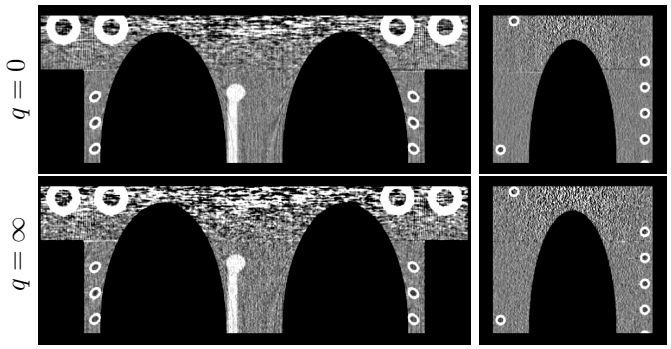

Fig. 1. ASSR, 16×1 mm collimation, 8 mm table increment. Coronal and sagittal MPRs of the thorax phantom. I2V using all planes ($q = 0$, top) vs. I2V using optimal planes only ($q = \infty$, bottom). Noise is increased by a factor of 1.7 for the latter case. (0/100)

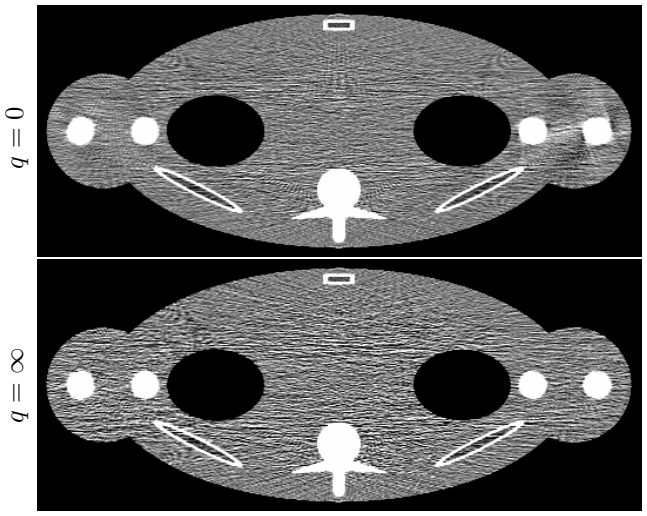

Fig. 2. ASSR, 16 × 1 mm collimation, $d = 8$ mm. The slices show a slight decrease of noise and an increase of artifacts when using all planes with equal weights ($q = 0$, top) in comparison to using only the optimal planes ($q = \infty$, bottom). (0/100)

VI. Results

In general, using non–optimal planes due to overlapping data acquisition shows no significant disadvantage as compared to the maximum pitch ($p = 1.5$) approach (original ASSR) except for the longer reconstruction time. This is demonstrated in figure 1 showing differences only in image noise which is increased by a factor of 1.7 for the reconstruction using only the optimal planes (this reconstruction is equivalent to a $p = 1.5$ scan with fewer slices). The increase in noise can be understood as follows: to achieve a table increment of 8 mm, a collimation of 5×1 mm would suffice (pitch 1.5). Thus, only 5/16–th of the detector are used by $q = \infty$ which is roughly $1/1.7^2$.

To demonstrate differences apart from the image noise between the ASSR approach only using the optimal planes ($q = \infty$) and the one making full use of the patient dose ($q = 0$) it is necessary to look at transaxial planes (as we have seen that no significant differences can be observed in MPR displays for the geometry we simulated). Therefore, figure 2 shows a slice in the shoulder region where attention should be paid to the four spheres representing the humerus. Especially one of the spheres is surrounded by artifacts for $q = 0$ whereas they are imaged artifact–free for the optimal $q = \infty$ case. A similar behavior can be observed for the ribs (no images shown). The streaks emerging from these spheres may lead to misdiagnosis: the real patient anatomy contains more complex objects close to the lung. An example may be the heart which is often filled with contrast agent. Making use of I2V's real–time capabilities and evaluating the volume as a function of q helps to resolve such ambiguities.

The reconstructions of our virtual heart phantom (phantom and motion function are defined in [11]) in figure 3 ($f_{\mathrm{H}} = 70$ min^{-1} and 130 min^{-1}) demonstrate the capability of I2V ASSR to resolve motion. We have chosen $q' = \infty$ for these reconstructions, except for the non–cardiac image which has been produced with $q' = 0$ to force equal weights for all planes. The images show optimal quality for low heart rates and less optimal quality for the high heart rate case. This is not surprising, since ASSR is a partial scan algorithm that makes use of 180° data always and its temporal resolution is $t_{\mathrm{rot}}/2$. In that respect, it is similar to the partial scan cardiac algorithm 180°MCD [11].

Reconstructions of the same data and the same slices using the multi-slice gold standard 180°MCI (Multi-slice Cardio Interpolation, images not shown here) are slightly superior due to the better temporal resolution of the multi–phase approach 180°MCI. However, 180°MCI is not suited for cone–beam scanners since 180°MCI does not take into account the cone–beam nature of the x–rays. To demonstrate this, we have reconstructed the thorax phantom in the cardio mode ($q' = \infty$) using ASSR and 180°MCI. The results (figure 4) show clearly the advantages of ASSR over 180°MCI. Especially in the humerus severe geometric distortions appear in 180°MCI. Some of the spheres appear to be egg–shaped. Artifacts are also apparent in the ASSR reconstruction. These are due to using only a few reconstruction positions ($q' = \infty$). In general, for ASSR no geometric distortions appear and the artifacts are less severe than for 180°MCI.

VII. Discussion

Our results indicate that there is no significant disadvantage of performing overlapping data acquisition and using non–optimal reconstruction planes instead of doing a high–pitch scan with optimal planes only. For transaxial planes, however, it seems to be of interest to be able to change the weight strategy on–line.

Of course, if the tube current is not the restricting factor of the scan, overlapping data acquisition should be avoided and the pitch should be set to 1.5, which is the optimal pitch for ASSR. Low pitch should be used only if one intends to accumulate dose to further decrease the image noise.

For the new cardiac approach, promising results can be obtained for the cardiac motion phantom within a wide range of heart rates.

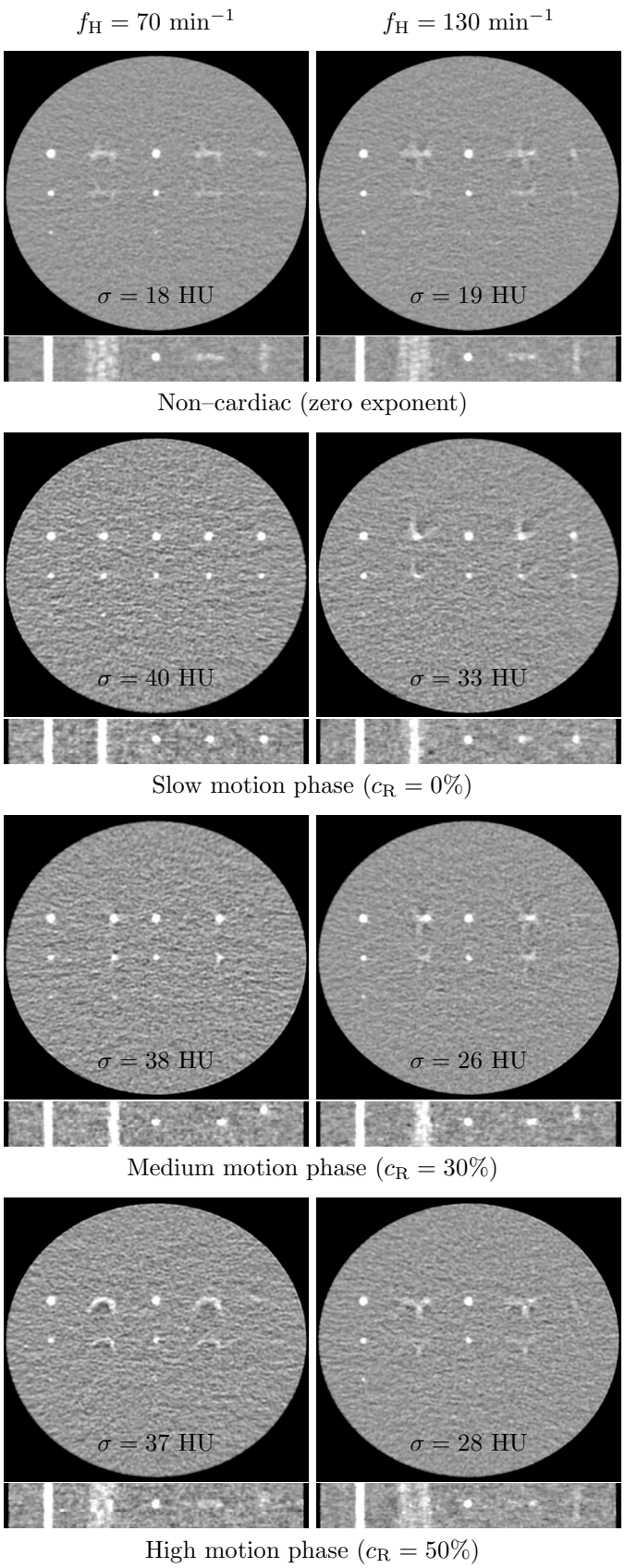

Fig. 3. ASSR for various weighting strategies and low (left column, 70 min^{-1}) and high (right column, 130 min^{-1}) heart rates. The MPRs extend over 17 mm in the z–direction and show the 3 mm calcifications. Image noise σ is given for a circular ROI centered in the lower heart region. (0/500)

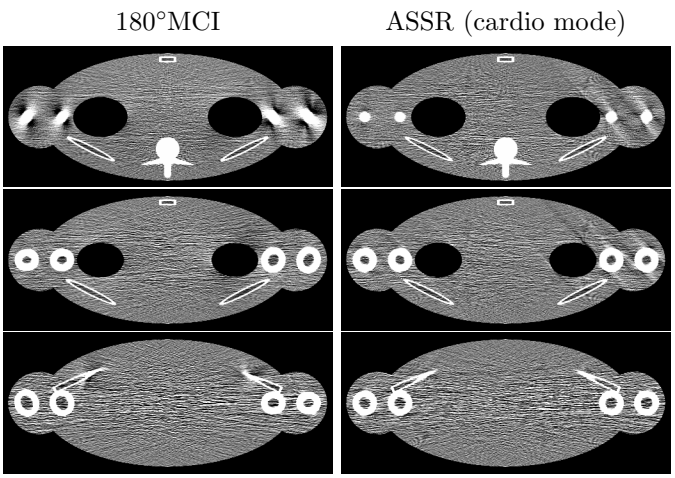

Fig. 4. 180°MCI and ASSR for $f_H = 70$ min^{-1}. (0/100)

The conclusions that can be drawn from a simulation study are restricted, however. The algorithms, the weighting strategies and the cardiac reconstruction will undergo further evaluation using real patient data and the expertise of radiologists.

Acknowledgements

This work was supported by grant AZ 262/98 of "Bayerische Forschungsstiftung, D–80333 München, Germany".

References

[1] W. A. Kalender, *Computed Tomography*. Wiley & Sons, 2000.
[2] H. Turbell, *Cone-Beam Reconstruction using Filtered Backprojection*. PhD Thesis, Linköping, 2001.
[3] M. Kachelrieß, S. Schaller, and W. A. Kalender, "Advanced single–slice rebinning in cone–beam spiral CT," *Med. Phys.*, vol. 27, pp. 754–772, Apr. 2000.
[4] F. Noo, M. Defrise, and R. Clackdoyle, "Single–slice rebinning method for helical cone–beam CT," *Phys. Med. Biol.*, vol. 44, pp. 561–570, 1999.
[5] G. Larson, C. Ruth, and C. Crawford, "Nutating slice CT image reconstruction apparatus and method," 1998. United States Patent 5,802,134.
[6] H. Bruder, M. Kachelrieß, S. Schaller, and T. Mertelmeier, "Performance of approximate cone–beam reconstruction in multi-slice computed tomography," *SPIE Medical Imaging Conference Proc.*, vol. 3979, pp. 541–555, 2000.
[7] H. Bruder, M. Kachelrieß, S. Schaller, K. Stierstorfer, and T. Flohr, "Single–slice rebinning reconstruction in spiral cone–beam computed tomography," *IEEE Transactions on Medical Imaging*, vol. 19, pp. 873–887, Sept. 2000.
[8] M. Kachelrieß, T. Fuchs, S. Schaller, and W. A. Kalender, "Advanced single–slice rebinning for tilted spiral cone–beam CT," *Med. Phys.*, vol. 28, pp. 1033–1041, June 2001.
[9] S. Schaller, K. Stierstorfer, H. Bruder, M. Kachelrieß, and T. Flohr, "Novel approximate approach for high-quality image reconstruction in helical cone beam CT at arbitrary pitch," *SPIE Medical Imaging Conference Proc.*, vol. 4322, pp. 113–127, 2001.
[10] M. Kachelrieß and W. A. Kalender, "Electrocardiogram–correlated image reconstruction from subsecond spiral computed tomography scans of the heart," *Med. Phys.*, vol. 25, pp. 2417–2431, Dec. 1998.
[11] M. Kachelrieß, S. Ulzheimer, and W. A. Kalender, "ECG–correlated image reconstruction from subsecond multi–slice spiral CT scans of the heart," *Med. Phys.*, vol. 27, pp. 1881–1902, Aug. 2000.
[12] M. Kachelrieß, S. Ulzheimer, and W. A. Kalender, "ECG–correlated imaging of the heart with subsecond multislice CT," *IEEE Transactions on Medical Imaging*, vol. 19, pp. 888–901, Sept. 2000.